

Supporting Information

Monodispersed Ag nanoparticles loaded on the PVP-assisted synthetic $\text{Bi}_2\text{O}_2\text{CO}_3$ microspheres with enhanced photocatalytic and supercapacitive performances

Shengjie Peng,^{*a} Linlin Li,^{a,b} Huiteng Tan,^a Yongzhi Wu,^{c,d} Ren Cai,^a Hong Yu,^{a,b} Xin Huang,^a Peining Zhu,^d Seeram Ramakrishna,^d Madhavi Srinivasan,^{a,b} and Qingyu Yan^{*a,b}

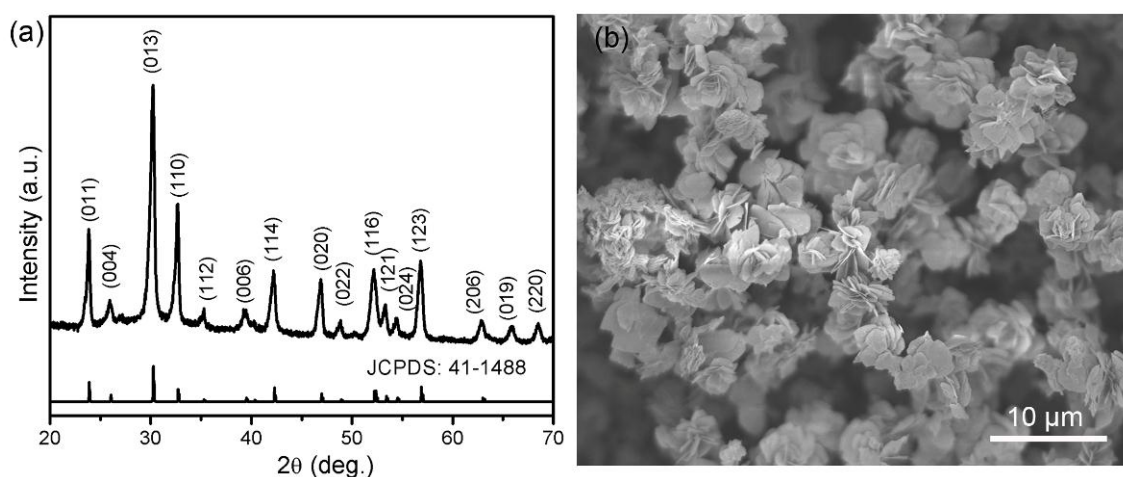


Fig. S1 XRD pattern and SEM image of the $\text{Bi}_2\text{O}_2\text{CO}_3$ -3 by using Na_2CO_3 as the precursor.

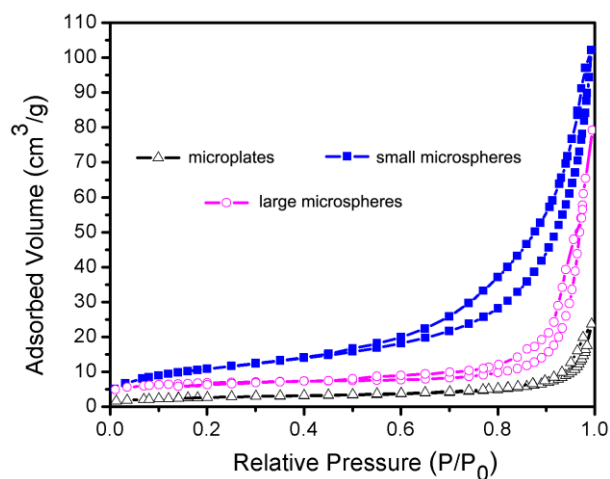


Fig. S2 Nitrogen adsorption–desorption isotherm and the corresponding pore size distribution (inset) of Bi₂O₂CO₃-1, Bi₂O₂CO₃-2 and Bi₂O₂CO₃-3, respectively.

The Brunauer–Emmett–Teller (BET) surface areas of Bi₂O₂CO₃-1, Bi₂O₂CO₃-2 and Bi₂O₂CO₃-3 calculated from N₂ isotherms are 45.8, 29.3 and 8.9 m² g⁻¹, respectively.

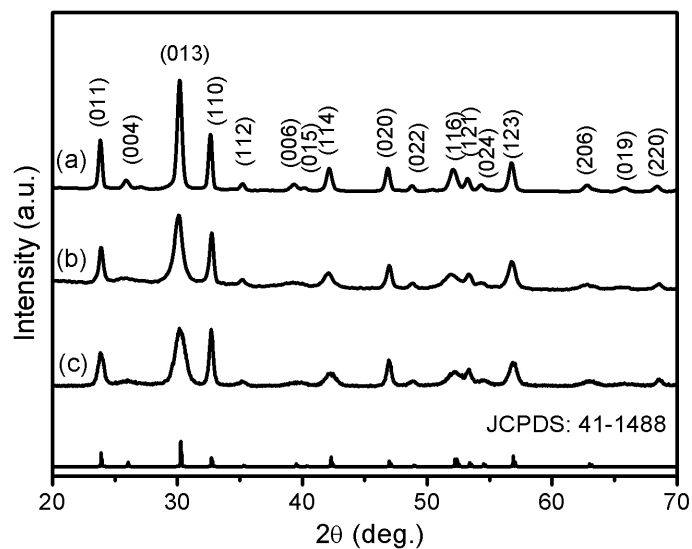


Fig. S3 XRD patterns of samples using different amounts of PVP: 0.2 g (a), 0.4 g (b), and 0.6 g (c), respectively.

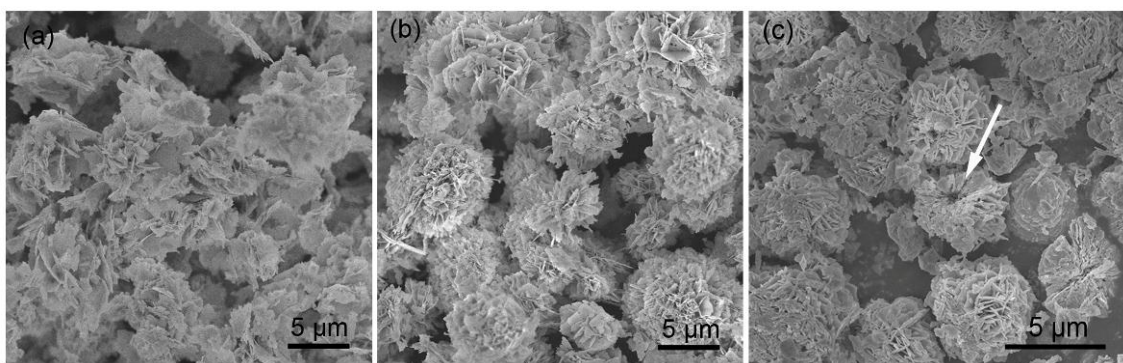


Fig. S4 SEM images of samples using different amounts of PVP: 0.2 g (a), 0.4 g (b), and 0.6 g (c), respectively.

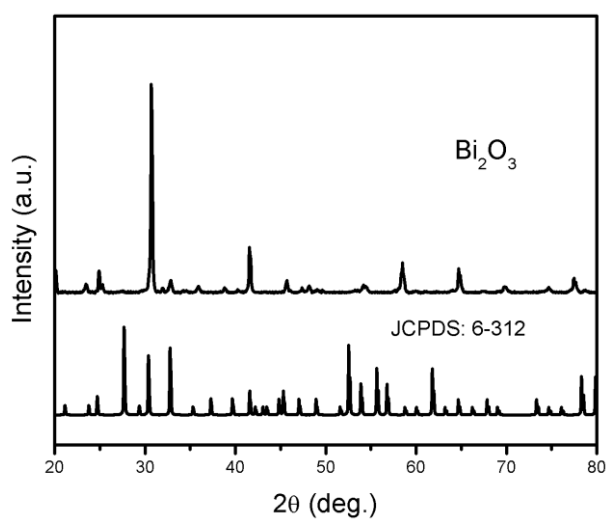


Fig. S5 XRD pattern of the product obtained in the absence of PVP and only using 0.9 g of HMT.

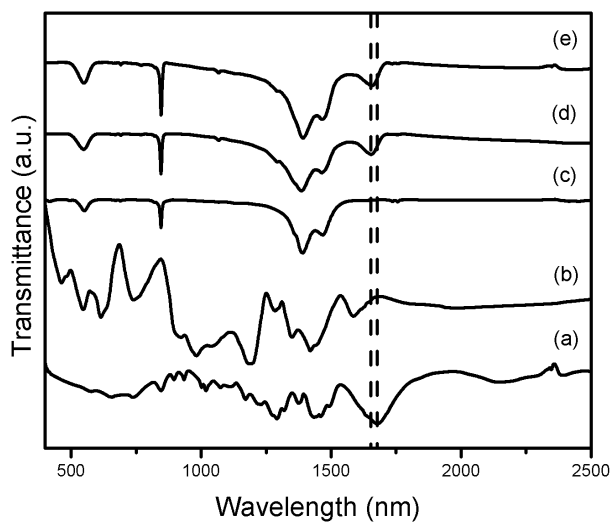


Fig. S6 IR spectra of the PVP (a), PVP/Bi(NO₃)₃ (b), Bi₂O₂CO₃-3 (c), Bi₂O₂CO₃-2 (d) Bi₂O₂CO₃-1 (e), respectively.

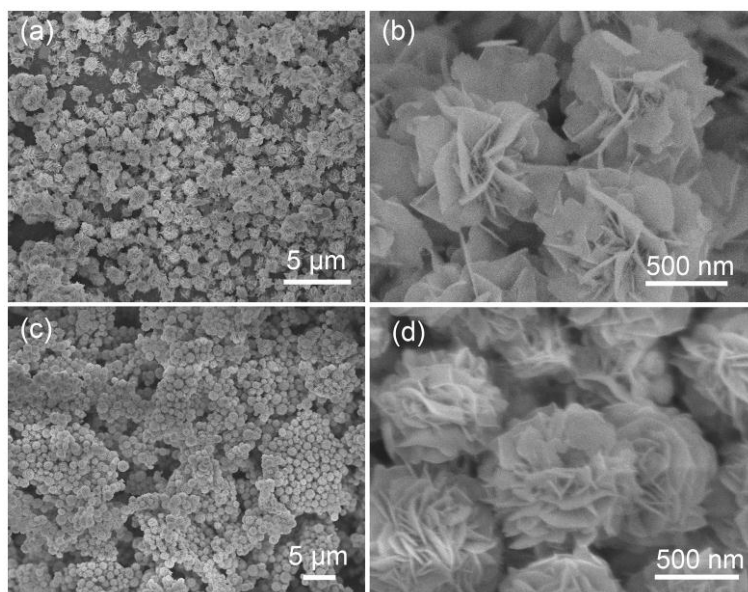


Fig. S7 SEM images of $\text{Bi}_2\text{O}_2\text{CO}_3\text{-1}$ obtained through different times: 30 min (a,b), and 4 h (c, d), respectively.

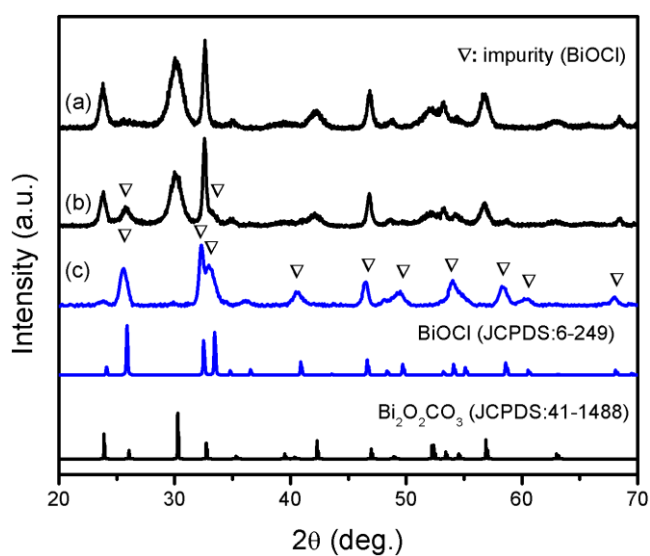


Fig. S8 XRD patterns of the products obtained by using 0.04 g (a), 0.06 g (b) and 0.2 g (c) of KCl, respectively.

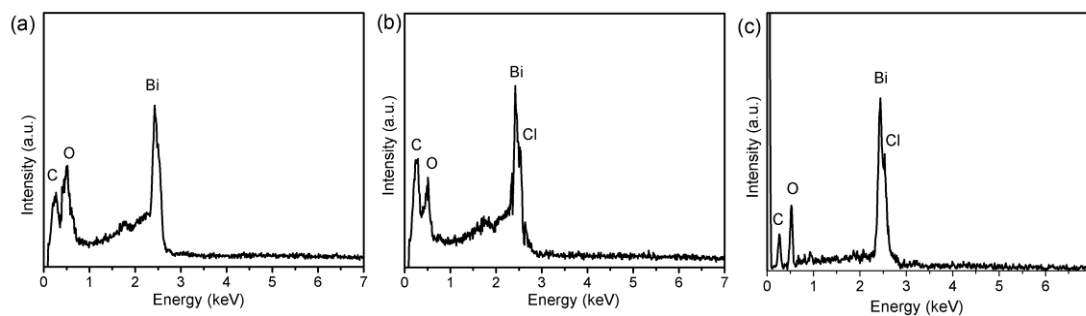


Fig. S9 EDS spectra of the products obtained by using 0.04 g (a), 0.06 g (b) and 0.2 g (c) of KCl, respectively.

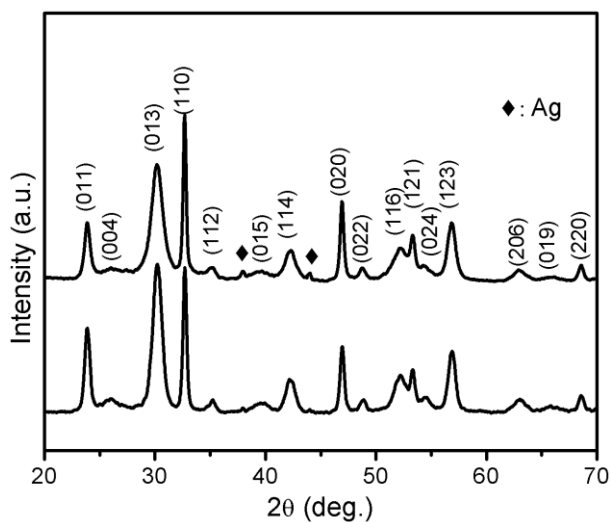


Fig. S10 XRD pattern of Ag(0.3%)/Bi₂O₂CO₃-1 and Ag(0.9%)/Bi₂O₂CO₃-1, respectively.

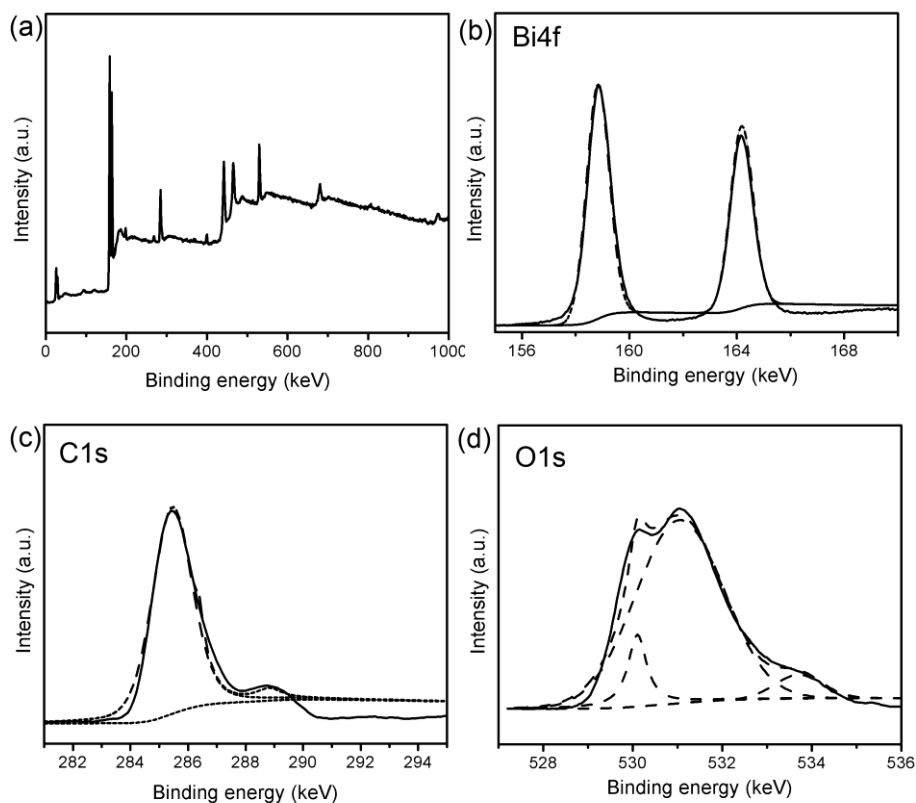


Fig. S11 XPS spectrum of the obtained Ag(0.6%)/Bi₂O₂CO₃-1: survey XPS spectrum (a), high-resolution Bi 4f (b), C 1s (c), and O 1s (d) spectrum.

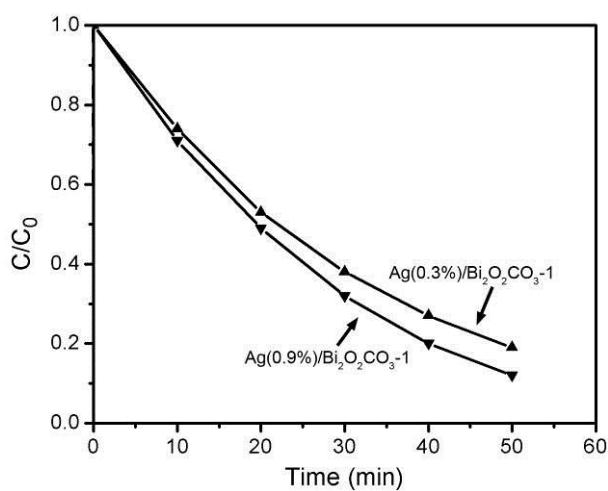


Fig. S12 Time-dependent absorption spectra of MO photocatalytic degradation with Ag(0.3%)/Bi₂O₂CO₃-1 and Ag(0.9%)/Bi₂O₂CO₃-1, respectively.

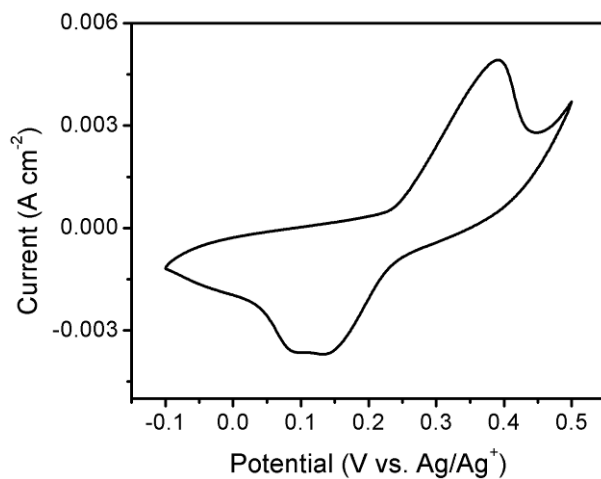


Fig. S13 The CV curves of Ni foam without loading of $\text{Bi}_2\text{O}_2\text{CO}_3$ at 50 mV s^{-1} .

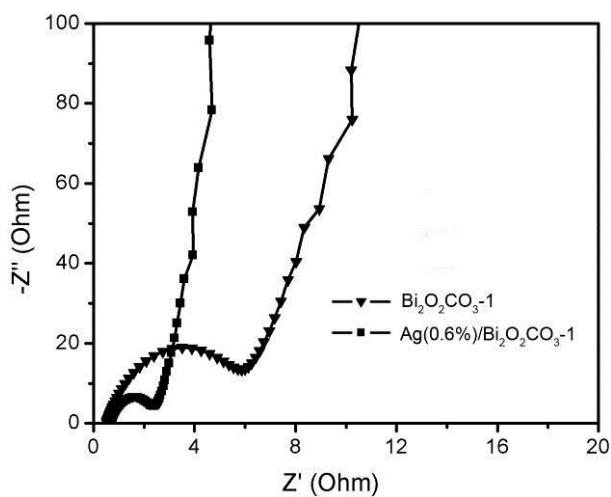


Fig. S14 Nyquist plots of the EIS for the $\text{Bi}_2\text{O}_2\text{CO}_3-1$, $\text{Ag}(0.6\%)/\text{Bi}_2\text{O}_2\text{CO}_3-1$.

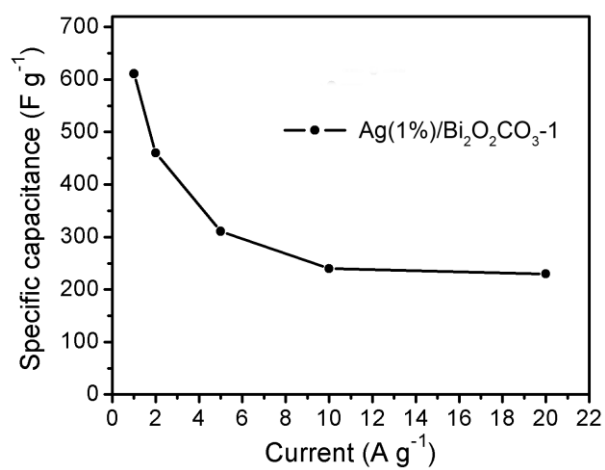


Fig. S15 Specific capacitance as a function of current densities for Ag(1%)/Bi₂O₂CO₃-1.